AIAA JOURNAL
Vol. 33, No. 8, August 1995

Minimal-Order Experimental Component Mode Synthesis: New Results and Challenges

K. F. Alvin,* L. D. Peterson,† and K. C. Park‡
University of Colorado at Boulder, Boulder, Colorado 80309-0429

An experimental component mode synthesis procedure is presented that consists of an objective substructure-level modal identification, a minimum-order substructure realization expressed in terms of physical displacement and residual modal coordinates, and a global synthesis that exploits the physical form of the substructure realizations. The present experimental procedure is analogous to and approaches in its asymptotic limit to the well-known Craig–Bampton analytical component mode synthesis but is motivated by the physical form of the minimal-order mass and stiffness representation. The procedure is illustrated in a step-by-step manner via a numerical example and then demonstrated by applying it to an experimental component mode synthesis of assembling two truss structures into a global structure.

Introduction

SYNTHESIS of an assembled structural model from a set of experimentally constructed substructure models remains a challenge to the structural dynamist. This is because, despite routine availability of finite/boundary element methods for discrete modeling of complex structures, significant discrepancies continue to exist between the discrete model and the laboratory-tested structural model. Such inadequacy in discrete structural models in capturing relevant dynamic characteristics observed in experiments can seriously hamper design improvements against vibrations either by passive isolation or active vibration control, if one utilizes only the analytical model. Thus, there is an increasing need for constructing experiment-based structural models, especially for high-performance and/or high-precision structures and equipment design.[1] Several technical issues, however, need to be resolved before the structural dynamist can routinely utilize an experimental component mode synthesis for constructing an assembled structural model from substructural realization models.

First, ambiguities abound in constructing each substructure model from test data, among practicing structural dynamists, through selection of an appropriate number of modes and their mode shapes. For example, correlation or reconciliation of finite element models to experimental data leads to difficult issues of uniqueness and convergence. Second, mode shapes chosen in each substructures may not be "in phase" relative to another; more precisely, the generalized coordinates of each substructure may not be transformed into a common global physical displacement coordinates. Third, in view of the present experimental capacity, one can now identify, for most cases, far more modes than the number of modes that meet orthogonality requirements given a limited number of sensors. Finally, the presence of noise and nonproportional damping in the measured data further complicate these three issues. It should be noted in passing that a parallel dilemma exists in analytical component mode synthesis such as the well-known Craig–Bampton technique.[2] For example, no adequate termination criterion exists for selecting the number of fixed interface modes without a repetitive convergence evaluation.

Several investigators have addressed issues pointed out in the preceding paragraph. Yang and Yeh[3] determine a mass and stiffness realization directly from a transformation of an identified continuous-time state space model, but this approach requires that both the number of force inputs and sensor measurements be equal to the number of identified modes, an impractical restriction. Su and Juang[4] offer a global synthesis that directly utilizes the substructure realizations in their first-order state space form. The global synthesis, however, is more cumbersome than simple mass and stiffness assembly and requires force inputs and sensor measurements at all interface degrees of freedom (i.e., those which must be compatible or in phase during synthesis). Martinez et al.[5] utilize a mass and stiffness representation consisting of the normal identified substructure modes complemented by residual flexibilities. To effect a global synthesis, the modal coordinates of each substructure are then transformed to a hybrid coordinate basis consisting of the common global interface degrees of freedom (DOF) augmented by nonphysical residual coordinates. The advantage of this approach is that it does not explicitly require force inputs at all interface DOF, although the accuracy of the residual flexibility terms at the interface are significantly affected by number and location of the inputs if they are to be estimated dynamically. It also allows all identified substructure modes to enrich the global model.

The objective of this paper is to offer a unified procedure that specifically addresses the minimal-DOF realization of each substructure in a common global basis, consisting of the static contribution of the measured substructure modes plus a minimal-order model enrichment of residual modes which are orthogonal to the static modes.[6] As such, the present procedure provides a mass and stiffness representation of each substructure possessing residual or augmented coordinates with a fixed-interface mode orientation similar to the Craig–Bampton technique. To this end, the paper is organized as follows. The first section briefly summarizes the relevant equations of motion and the determination of normal modes, which are central to the present procedure. The next section describes step-by-step the experimental design requirements and analytical synthesis procedure that results in a global mass and stiffness model of the assembled structural system. This procedure is then illustrated through a numerical example utilizing two spring-mass components. The experimental component model synthesis test is then summarized in terms of the experiment design and the synthesis results. Finally, concluding remarks are offered and analytical details are provided in the appendices.

Identification of Normal Modes from Test

System identification for flexible structures generally utilize frequency-domain transfer function (FRF) estimates over the bandwidth of interest for each input–output pairing, obtained through white-noise input forces, discrete Fourier transform methods, and

Presented as Paper 94-1570 at the AIAA/ASME/ASCE/AHS/ASC 35th Structures, Structural Dynamics, and Materials Conference, Hilton Head, SC, April 18–20, 1994; received May 2, 1994; revision received Dec. 14, 1994; accepted for publication Dec. 14, 1994.

*Research Associate, Center for Aerospace Structures and Department of Aerospace Engineering Sciences. Member AIAA.

†Assistant Professor, Center for Aerospace Structures and Department of Aerospace Engineering Sciences. Senior Member AIAA.

‡Professor, Center for Aerospace Structures and Department of Aerospace Engineering Sciences. Associate Fellow AIAA.

ensemble averaging.[7,8] Modal parameters are then obtained either by curve fitting techniques or from an equivalent system realization of the data in the time or frequency domain. The eigensystem realization algorithm[9] (ERA) is a system realization method in the time domain that has become popular in recent years, particularly with respect to identification of structural dynamic systems. ERA will identify a minimum-order discrete-time model to approximate the discrete system impulse response using numerical techniques that are robust in the presence of repeated roots and measurement noise.

Often, the reconstruction of measured response from the time-domain system realization is too inaccurate for application of physical transformation and synthesis-based algorithms. One particular source of inaccuracy is the presence of modes above the test bandwidth when acceleration sensors are utilized. This is because the discrete linear first-order realization theory cannot correctly model the influence of these modes on inertance data. This can be alleviated through a frequency domain re-estimation of the state space output coefficient arrays and inclusion of a continuous-time nonproper term which models the high-frequency mode contribution within the measurement bandwidth.[10]

The discrete-time state space portion of the realization can then be converted to a corresponding set of continuous time equations, viz.,

$$\begin{aligned} \dot{x} &= Ax + Bu \\ y &= Cx + Du \end{aligned} \tag{1}$$

where x is the N-length dynamic state vector, u is the m-length force input vector, y is the l-length vector of measured outputs, A is the $N \times N$ state transition matrix, B is the $N \times m$ input influence matrix, C is the $l \times N$ output influence matrix, and D is the $l \times m$ input–output feedthrough matrix, respectively. Although Eq. (1) is strictly a mathematical representation of the characteristic impulse response functions of the structure, certain physically based structural synthesis techniques are possible given that the sensor measurements $y(t)$ can be related to physical degrees of freedom in a structural model.

The modal parameters of second-order dynamics are then extracted from the state space equations. The associated second-order equations of motion for structural dynamics are generally given as

$$M\ddot{q} + D\dot{q} + Kq = \hat{B}u \tag{2}$$

where M, D, and K are the mass, damping, and stiffness matrices, respectively, q is a n vector of displacement variables, u is the m-vector of input forces, and $\hat{B}$ maps u to the physical degrees of freedom q. The associated normal modes are defined by the generalized undamped eigenproblem

$$K\Phi_n = M\Phi_n\Omega \tag{3}$$

$$\Phi_n^T K \Phi_n = \Omega = \left\{\omega_{ni}^2, i = 1, \ldots, n\right\}$$

$$\Phi_n^T M \Phi_n = I_{n\times n} \tag{4}$$

$$\Phi_n^T D \Phi_n = \Xi$$

where Φ_n are the mass-normalized mode shapes of K and M, Ω is a diagonal matrix of undamped eigenvalues (which are the squares of the natural frequencies ω_{ni}), and Ξ is the modal damping matrix. These real modal parameters of the second-order system can be related to the complex eigenmodes of Eq. (1) by either rule-of-thumb approximations or transformation-based procedures.[11,12]

Minimal-Order Experimental Component Mode Synthesis

The present unified procedure for experimental component model synthesis (CMS) is described subsequently. First, the experiment design requirements will be reviewed. Then, the model identification and analytical synthesis step will be given in detail.

Experimental Design for Component Model Synthesis

The analytical synthesis of the experimental component realizations is based on the properties of the mass-normalized normal mode shapes at the interface DOF and the estimated undamped modal frequencies of each identified component. To this end, the following are key necessary experiment design requirements for the present procedure.

1) Component-to-component interfaces on each structure must be unconstrained, along with all other interfaces not fixed to ground in the assembled structure. This implies that components which are only constrained globally through their assembly to other components should be tested in a free-free state, or constrained only through suspension systems which do not interact with the component free-free dynamic modes.

2) Sensor measurements are required for all primary interface degrees of freedom. The sensors must provide either displacement, velocity, or acceleration output, such that either directly or through integration they provide a measure of the displacement mode shapes at the interface. Depending on the interface redundancy, rotational sensor measurement may or may not be required; often rotational DOF can be estimated from spatial integration using other sensors.

3) One or more measured force inputs must be used to excite the disturbable intrinsic component modes. Ideally, these inputs should be applied on or close to the interfaces, such that all modes observable from the interface within the measurement bandwidth are accurately characterized. The use of two or more inputs allows the discrimination of repeated modes in a structure possessing cyclical symmetry.

4) Independent collocated displacement-based (i.e., displacement, velocity, or acceleration) sensor measurements must be in line with the force inputs. These are the so-called driving point measurements that allow the correct physical normalization of the identified mode shapes. For free components, the mass-normalization of the rigid-body modes will also require knowledge of the system mass and moments of inertia.

5) Ideally there will be a high-measurement bandwidth that includes both the important "global" modes of the component and localized vibrational modes near the component interfaces.

Before proceeding, we offer the following observations. The requirements are not unusual and can generally be satisfied by standard modal testing procedures. The particular need of sensing interfaces, however, should be closely followed. In addition, the use of numerous inputs is recommended. This is because, although mass-normalized mode shapes allow reconstruction of both point and transfer flexibility terms, only the modes in the bandwidth may be so treated. For modes outside the measurement bandwidth, only their sum contribution to flexibility can be estimated, and so a greater number of inputs allows for greater accuracy in the determination of flexibility and, thus, component stiffness.

Component Identification and Global Synthesis

The analytical procedure described herein is a physically motivated approach utilizing the mass-normalized component modes and mode shapes and their relationship to the component mass and stiffness. Our method has a direct analog in the component mode synthesis of analytical structural models,[13] the Craig-Bampton dynamic substructuring technique.[2] The two approaches are mathematically distinct, however, and only correspond exactly in the limiting case where both use the full set of normal modes which span the component dynamics. The present experimental method proceeds as follows.

1) Identification is made of an accurate discrete-time or continuous-time multiple-input-multiple-output (MIMO) realization of the measured component frequency response functions. Each component test may be individually treated. Algorithms such as ERA and Polyreference have been found to be effective in obtaining accurate minimal-order system realizations. In addition, some algorithms allow frequency-domain identification or adjustment of modal vectors and yield estimates of the residual flexibility of modes outside the testing bandwidth.[10]

Table 1 Comparison of frequencies for numerical example

Frequency exact model, Hz	Frequency identified/ synthesis, Hz	Error, %
0.2497	0.2495	−0.10
0.7431	0.7388	−0.57
1.2181	1.2220	0.32
1.6632	1.6632	0.004
2.0673	2.0684	0.054
2.4204	2.4209	0.019
2.7140	2.7140	−0.001
2.9408	2.9409	0.003
3.0951	3.0951	−0.0003
3.1733	3.1733	−0.0004

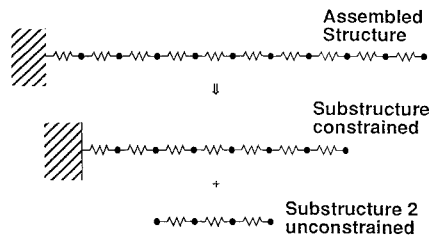

Fig. 1 Spring-mass system numerical example.

2) Determination or extraction of the mass-normalized real mode shapes and undamped natural frequencies and damping ratios is next. This was discussed in the preceding section. d

3) The so-called minimal-order mass and stiffness realization for each component is constructed. This realization is of a minimal order so as to equivalently represent both reduced mass and stiffness[14] at the measured component interface and the complete set of identified component modes and their mode shapes. The analytical procedure is detailed in Appendix A of this paper.

4) Global synthesis of the individual minimal-order mass and stiffness component models into the coupled system by direct displacement-based matrix assembly (equivalent to finite element global assembly of substructures) is the last procedure. This step is detailed in Appendix B of this paper.

In the following section, these procedural steps will be illustrated through a numerical example of a spring-mass system.

Numerical Example

Figure 1 illustrates a simple 10 DOF mass-spring system which is partitioned into a constrained and an unconstrained pair of substructures. The discrete impulse response of each substructure is simulated with 1% noise and identified using efficient system realization techniques.[15] Then, using the minimal-order mass and stiffness procedure, each substructure identification yields the desired Craig–Bampton mass and stiffness matrices. For conservatism, a number of noise modes (interpreted on the basis of their respective modal quality indicators) were included in the derivation of the minimal-order mass and stiffness. This is to ensure that their inclusion in the case of real data does not significantly degrade the quality of the global synthesis. Finally, assembling the global model through the displacement compatibility and equilibrium constraints, the global modes were obtained at the physical DOF which form the union of the measured sensors from the substructure responses. Computing the modal assurance criteria between the identified/synthesized mode shapes and the corresponding exact modes, the modes of the global synthesis model corresponding to the exact modes of the global system were identified. The results in terms of error in estimated frequency are shown in Table 1.

Substructure Identification Experimental Testbed

The experimental testbed structure consists of a 2-m 4-bay cantilevered truss tower and a 3-bay truss appendage substructure as shown in Fig. 2. Phase A of the experimental testing characterized the dynamics of the tower substructure (Fig. 3) and the appendage (Fig. 4). Phase B was then a test of the global structural

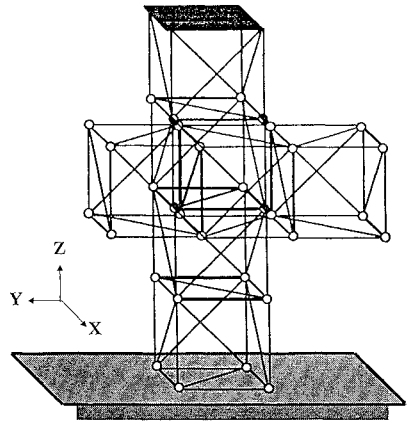

Fig. 2 Coupled structure test configuration.

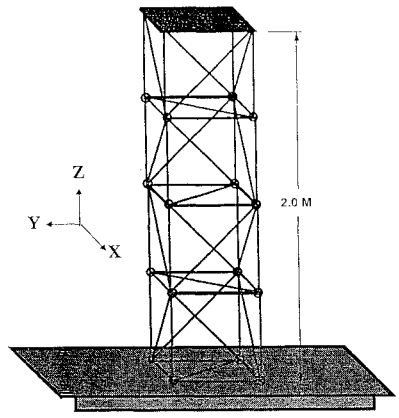

Fig. 3 Cantilever tower substructure.

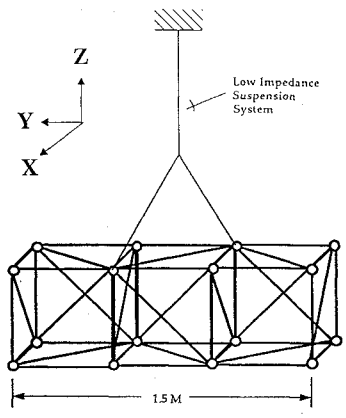

Fig. 4 Suspended substructure assembly.

configuration, where the appendage is mounted to the structure through four offset fittings, as illustrated in Fig. 5. Figure 6 shows the actual laboratory testbed substructures. It should be noted that, although the testbed and the numerical example both consist of one constrained and one unconstrained structure, this is coincidental and not a requirement or limitation of the method.

The testbed configuration has been designed to demonstrate the basic feasibility of the substructure identification synthesis approach. As such, issues of dynamic simplicity (e.g., cantilevered constraint) and complexity (e.g., joint dominated structure with localized dynamics) must be balanced. Nonetheless, even a structure with relative dynamic simplicity poses a number of significant experimental challenges to be overcome in order to effect an accurate model synthesis.

Interface Design and Measurement

Redundant hardware (e.g., joint fittings) at component interfaces are not easily isolated in substructure identifications. Interfaces

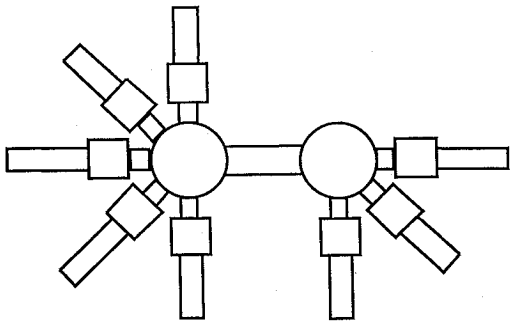

Fig. 5 Substructure interface connection.

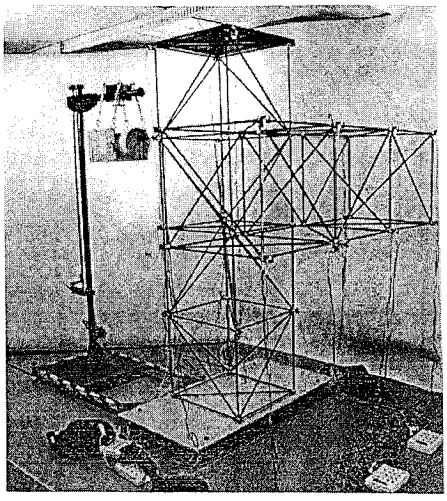

Fig. 6 Assembled structure during testing.

must, however, remain structurally stable in the substructure configuration. In addition, compatibility requires that interface DOF be measured directly at the coincident DOF on each substructure. This is complicated by the use of triaxial sensor blocks, which are offset from the structural load paths.

Free-Free Substructure Dynamics

Typically, individual substructure dynamics include rigid-body modes, which are either constrained in test (e.g., Fig. 4), or are not accurately measurable dynamically if they are unconstrained. However, substructure model synthesis requires accurate knowledge (including mass normalization) of the rigid-body modes. Fortunately, knowledge of the rigid-body mass properties allows the analytical synthesis of these modes.

Dynamic Measurement of Interface Stiffness

Both global and local modes contribute to the construction of interface stiffness, and thus local mode identification accuracy can become important to the success of substructure identification synthesis. Its importance is relative to the nature of the modes in the global structure; that is, the lowest modes of the assembled structure require less knowledge of the local mode contributions of the substructures. Conversely, the dynamics near the substructure I/F require more accurate identification of the local substructure dynamics in that region.

Driving-Point Normalization of Identified Modes

To effect a truly finite element model-independent synthesis of the substructure identifications, it is necessary to determine the correct mass normalization of the identified mode shapes independent of an assumed analytical mass matrix. This can be accomplished by an accurate driving-point (i.e., collocated with input force) acceleration measurement. Figure 7 illustrates the mechanical design employed in the present testing scenario. A shear accelerometer is mounted in line with the shaker force applied through a stinger. A structural cage

Table 2 Comparison of phase A tower test to NASTRAN model

Mode number	NASTRAN frequency, Hz	Test-identified frequency, Hz	Test-identified damping ratio, %
1 ($+X - Y$ bend)	12.177	11.529	0.78
2 ($+X + Y$ bend)	13.080	12.846	0.18
3 (1st torsion)	46.727	47.935	0.09

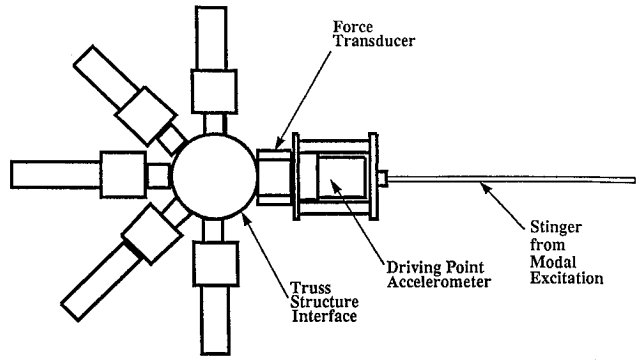

Fig. 7 Driving point measurement setup.

distributes the applied load around the accelerometer, effectively isolating the device. The force transducer, also mounted in-line, measures the actual dynamic applied loading, and thus the cage and stinger stiffness does not affect the measured response functions from test.

Phase A Test Results

The individual substructure modal tests were performed with 8192 samples per ensemble at a sampling rate of 500 Hz and averaged over 50 trials. For both tests, a single input was applied to identify the substructural modes. This is in strong contrast to applying inputs at all interface-compatible DOF, a necessary test criterion for nondisplacement-based synthesis methods.[4] The FastERA algorithm[15] was then use to determine a series of state space realizations of the measured FRFs which optimally matched the first 40 Markov parameters for particular model orders from 48 to 400 states. For the tower component, a system realization of order 248 was reduced through discarding inaccurate modes to a final order of 112, corresponding to 56 normal modes. For the suspended truss, a realization of order 328 was reduced to 94 states, corresponding to 47 normal modes. These model choices were arrived at by compromising convergence of the localized modes and divergence of the global modes (due to pole splitting). The system realizations were reduced by eliminating real poles and unstable poles and modes with low-accuracy indicators. The substructure identifications were finally refined by frequency-domain curve fitting which yields both the modal vectors and a measure of the residual stiffness of modes outside the bandwidth.[10] Table 2 lists the preliminary analysis and test results for the 4-bay tower substructure testing. Figures 8 and 9 illustrate typical inertance FRFs measured from the test and the final model reconstructions of the response for the tower and 3-bay components.

Experimental Synthesis and Phase B Test Results

To synthesize the global structural model from the individual substructure identifications, the minimal-order mass, damping, and stiffness matrices were determined from the free interface modes of the substructures. For the suspended 3-bay truss, a mass properties analysis, corroborated by the measured mass, was used to compute the six rigid-body modes. For example, the mode shape of the rigid-body X-translation mode is a unit displacement of all X DOF divided by the square root of the total mass, and zero elsewhere. The rotational rigid-body modes require knowledge of the total substructure rotational inertia. Finally, for both structures, eigenvector transformation matrices (ETM) were computed that reconstruct the

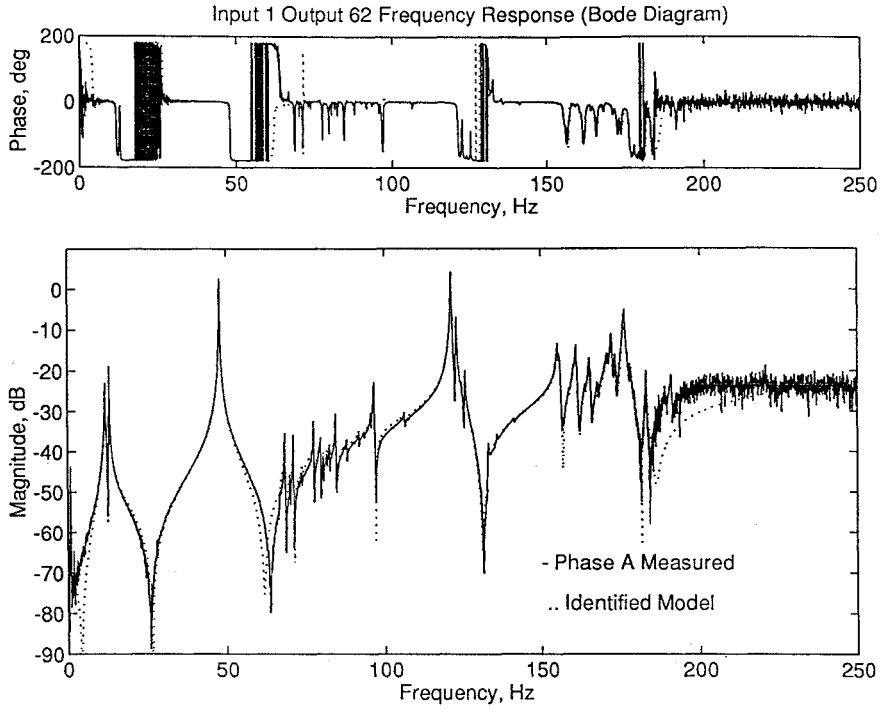

Fig. 8 Measured FRF and reconstruction for tower.

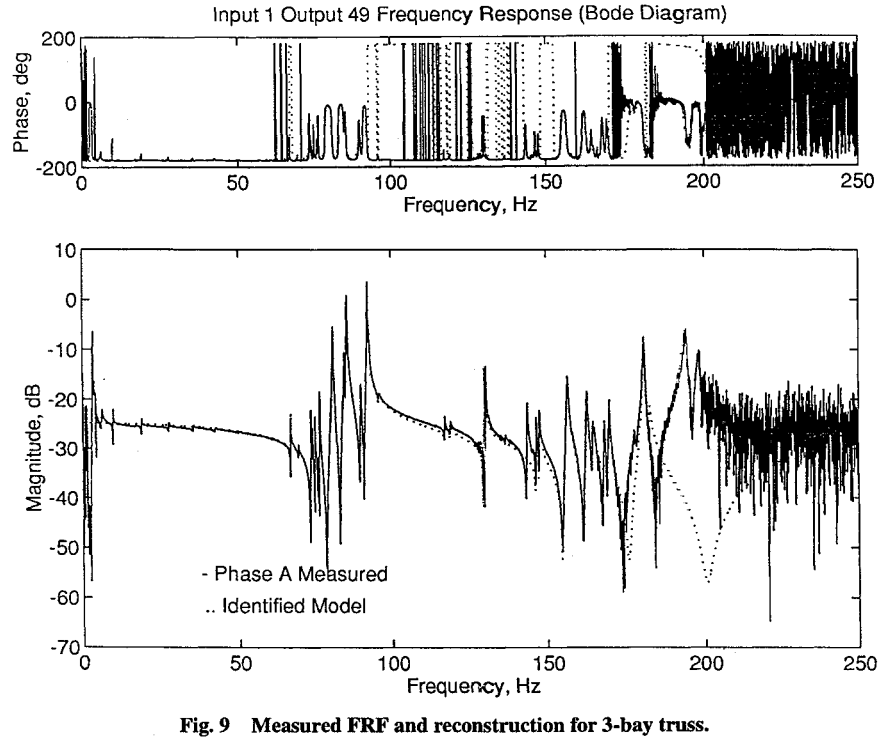

Fig. 9 Measured FRF and reconstruction for 3-bay truss.

displacement response of any measured DOF on either substructure as a function of the physical boundary displacements and generalized fixed interface modal displacements. Through the ETMs, mode responses on the global structure can be predicted anywhere substructure sensors were located.

Table 3 compares the lowest four modes of the CMS-synthesized model with an identification of the phase B (global structure) modal test. Table 3 also lists the damping ratios as identified from the test and synthesized from the substructure tests. Note that the experimental CMS procedure can also be applied to the component damping matrices. Figure 10 illustrates the measured driving point inertance and final identified model reconstruction for the global coupled structure. To compare the relative similarity of the synthesized mode shapes to the phase B test-identified modes, the modal assurance criteria (MAC) is computed as

$$\mathrm{MAC}_{ij} = \frac{\left(\phi_i^T \phi_j\right)^2}{\left(\phi_i^T \Phi_i\right)\left(\phi_j^T \phi_j\right)} \tag{5}$$

where ϕ_i and ϕ_j are mode shapes obtained from the experimental component mode synthesis analysis and the identification of the assembled structure, respectively.

Figure 11 illustrates a contour plot of the modal assurance criteria between the lowest 10 modes of the synthesis model and the test-identified modes. As can be seen, only the lowest three

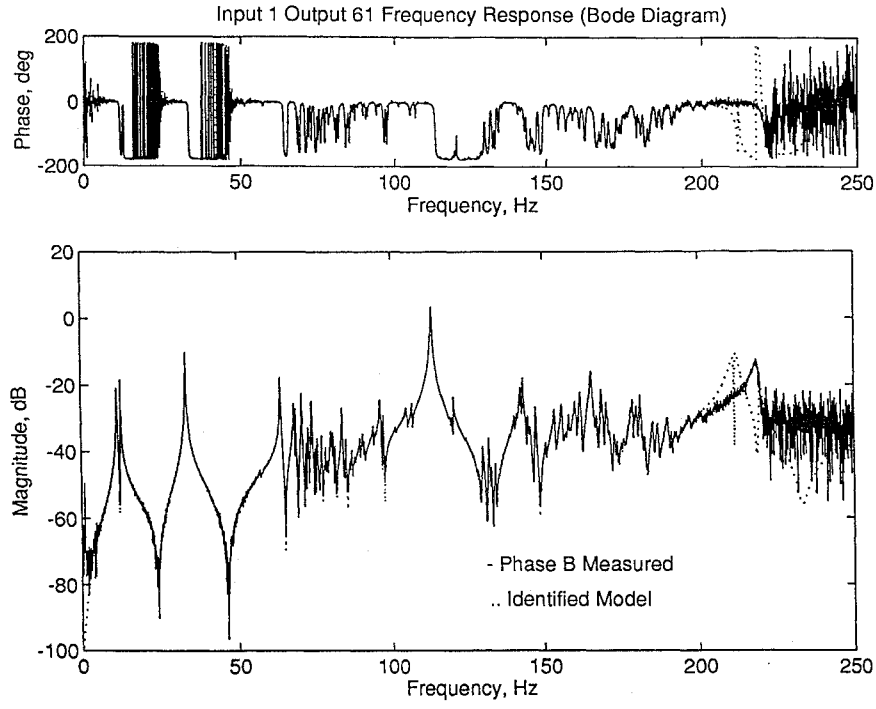

Fig. 10 Measured FRF and identification for global structure.

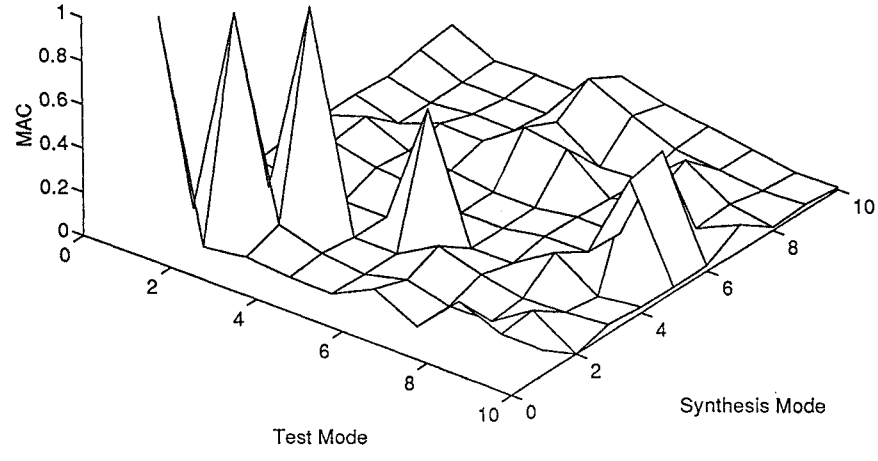

Fig. 11 Comparison of modal assurance criterion array.

Table 3 Comparison of substructure identification and CMS method to phase B test

Mode number	Substructure CMS synthesized, (%)	Test identified, (%)	MAC
1	11.221	11.273	0.980
	(0.759)	(0.576)	
2	12.566	12.485	0.981
	(0.176)	(0.185)	
3	36.207	33.400	0.986
	(0.062)	(0.195)	
4	56.899	63.985	0.571
	(0.082)	(0.170)	

"global" modes were successfully synthesized by the substructure CMS method as indicated by correlation between the mode shapes. Figure 12 compares the singular values at each frequency of the multiple output set of inertance FRFs. Note that although the numerous local modes were not effectively reconstructed by the substructure CMS method, the mean response behavior of the system was effectively obtained. Note also that another global mode response at around 113 Hz, the second bending of the tower in the $X-Z$ plane, was also identified by the synthesis method. The antialias filtering of the sensors in each test effectively limits the measurement bandwidth to 185 Hz; thus, the response above this limit was not fit in either the substructure tests or the global test.

The experimental testbed results are encouraging given the numerous restrictions posed by experimental design. For example, the interface stiffness which is critical to the global synthesis is determined strictly from contributions of the identified modes within the measurement bandwidth. It is well known, however, that stiffness contributions from higher frequency modes may be important, particularly when shear deformations of the interface dominate the global mode. An accurate measure of the residual flexibility due to these modes can only be obtained for measured DOF with respect to the input location. Because this flexibility is a single sum total value for each response, it cannot be decomposed and normalized into modes to reconstruct for other input locations. Furthermore, by using a single input, repeated modes could not be determined. In the case of the local modes in the region of 60–100 Hz in the tower and throughout the 3-bay component it is likely there are numerous repeated modes that could not be individually characterized from single-reference FRF data.

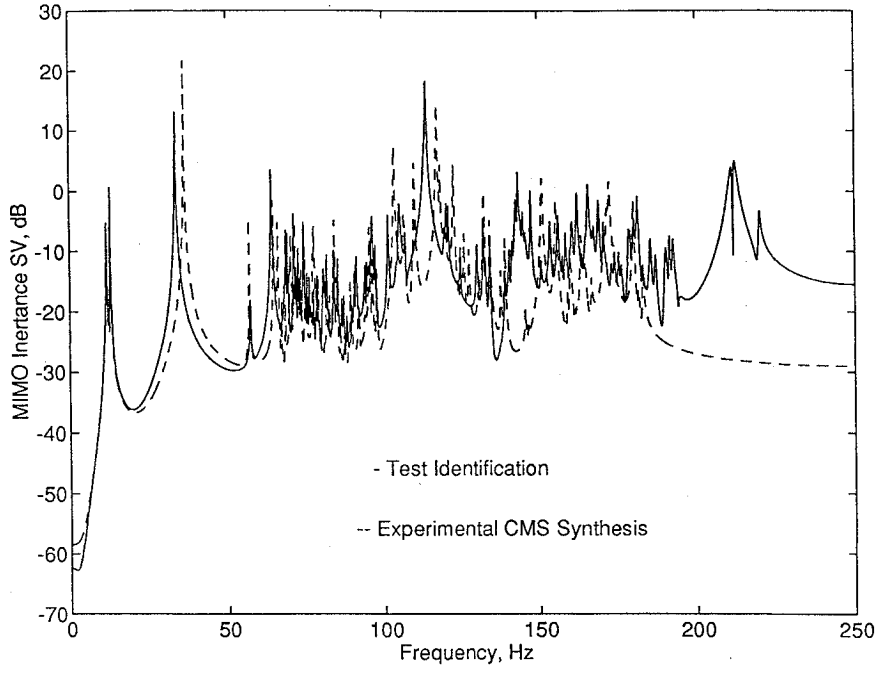

Fig. 12 Comparison of inertance FRF singular values.

Conclusions

An experimental component mode synthesis procedure has been presented that uses identifications of individual components. Then, through equivalent mass and stiffness representations of the components, a global model of the coupled structural dynamics is assembled. The present procedure relies on accurate measurement of the component interface DOF and driving-point measurements of the inputs to mass normalize the identified mode shapes of the components. The procedure has been illustrated through a numerical example and results from an experimental truss structure testbed. The synthesis correctly determined the first three global modes of the assembled structure, together with rough damping estimates, without reliance on any pre-existing finite element models. Poorer results for the localized dynamics indicate that much additional accuracy can be accrued by improvements in residual stiffness estimation at the interfaces. We hope to address these new challenges in our future work.

Appendix A: Construction of Minimal-Order Substructure Mass and Stiffness Matrices

In this section, we review a method for constructing reduced-order and minimal-order mass and stiffness matrices[6] directly from measured normal modal parameters that have asymptotic equivalence to existing finite element model reduction and synthesis methods. We begin by developing the concept of reduced mass and stiffness matrices, which are defined with respect to only the sensor DOF.

If we partition the DOF of a large-order structural dynamics model such as those obtained from finite element discretization into sets m and i, we have

$$\begin{bmatrix} M_{mm} & M_{mi} \\ M_{mi}^T & M_{ii} \end{bmatrix}\begin{bmatrix} \ddot{q}_m \\ \ddot{q}_i \end{bmatrix} + \begin{bmatrix} D_{mm} & D_{mi} \\ D_{mi}^T & D_{ii} \end{bmatrix}\begin{bmatrix} \dot{q}_m \\ \dot{q}_i \end{bmatrix} + \begin{bmatrix} K_{mm} & K_{mi} \\ K_{mi}^T & K_{ii} \end{bmatrix}\begin{bmatrix} q_m \\ q_i \end{bmatrix} = \begin{bmatrix} \hat{B}_m \\ \hat{B}_i \end{bmatrix} u \tag{A1}$$

where M, D, K, q, and u are as defined in Eq. (2). Then solving the static equations where no forces are applied to the q_i equations ($\hat{B}_i u = 0$), we have

$$q_i = -K_{ii}^{-1} K_{mi}^T q_m \tag{A2}$$

and a variable reduction operator is given as

$$\begin{bmatrix} q_m \\ q_i \end{bmatrix} = \begin{bmatrix} I \\ -K_{ii}^{-1} K_{mi}^T \end{bmatrix} q_m = \Phi_c q_m \tag{A3}$$

In component mode synthesis (CMS) theory, Φ_c are often termed the constraint modes, as they represent the displacement vectors of the internal DOF q_i with respect to the constraint modes, defined as the set of orthogonal unit displacements of the retained degrees of freedom q_m. Applying the transformation in Eq. (A3) to K, D, and M in Eq. (A1), the so-called Guyan reduced stiffness, damping, and mass[14] are

$$\bar{K} = \Phi_c^T K \Phi_c = K_{mm} - K_{mi} K_{ii}^{-1} K_{mi}^T \qquad \bar{D} = \Phi_c^T D \Phi_c \qquad \bar{M} = \Phi_c^T M \Phi_c \tag{A4}$$

Alternately, if we express the physical degrees of freedom q in terms of the normal modal variables η, we have the transformation

$$q = \Phi_n \eta = \begin{bmatrix} \phi_m \\ \phi_i \end{bmatrix} \eta \tag{A5}$$

where ϕ_m and ϕ_i are partitions of the mass-normalized eigenvectors at the measured and unmeasured (i.e., internal) DOF, respectively. Using Eq. (4) and assuming no rigid-body modes, a solution to the inverse vibration problem is given by

$$\bar{K} = \left[\phi_m \Omega^{-1} \phi_m^T\right]^{-1}$$
$$\bar{M} = \bar{K} \phi_m \Omega^{-2} \phi_m^T \bar{K} \tag{A6}$$
$$\bar{D} = \bar{K} \phi_m \Omega^{-1} \Xi \Omega^{-1} \phi_m^T \bar{K}$$

The reduced system matrices given by Eq. (A6) are theoretically consistent with the Guyan reduction in the limit as the full eigenspectrum of Eq. (2) is measured. In addition, they are a function only of the partition of the mode shapes at the measured locations and, thus, can be directly calculated from the measured test data. Modifications are necessary to this procedure in order to accommodate rigid-body modes; details can be found in Ref. 6.

The determination of minimum-order equivalent mass and stiffness from a test is based on the Craig–Bampton component mode synthesis method,[2] which itself is related to the statically condensed mass and stiffness of the Guyan reduction. As such, we will use the

method of determining the Guyan reduction from measured modes as just reviewed to develop the equivalent minimum-order method.

Starting from $\bar{K}$ we can construct minimal-order stiffness and mass matrices $\hat{K}$ and $\hat{M}$, respectively, from the measured modal test parameters ϕ_m and Ω as follows. Partition the eigenvectors of $\hat{K}$ and $\hat{M}$ as

$$\hat{K}\begin{bmatrix}\phi_m\\ \phi_{\text{res}}\end{bmatrix} = \hat{M}\begin{bmatrix}\phi_m\\ \phi_{\text{res}}\end{bmatrix}\Omega \tag{A7}$$

where

$$\hat{K} = \begin{bmatrix}\bar{K} & 0\\ 0 & \Omega_{\text{res}}\end{bmatrix} \qquad \hat{M} = \begin{bmatrix}\bar{M} & M_c\\ M_c^T & I\end{bmatrix} \tag{A8}$$

are the Craig–Bampton CMS stiffness and mass matrices, respectively, and the associated mode shapes are normalized such that

$$\begin{bmatrix}\phi_m^T & \phi_{\text{res}}^T\end{bmatrix}\hat{K}\begin{bmatrix}\phi_m\\ \phi_{\text{res}}\end{bmatrix} = \Omega \tag{A9}$$

Here, ϕ_{res} are the partition of the eigenvectors of $\hat{K}$ and $\hat{M}$ relating a set of augmented variables ξ to the normal modal variables of the global system η. Although ϕ_{res} and Ω_{res} are unknowns, together they form a dynamic residual matrix $\Delta\Omega$ which can be computed by the test-measured quantities ϕ_m, Ω, and $\bar{K}$, viz.,

$$\begin{aligned}\Delta\Omega &= \phi_{\text{res}}^T\Omega_{\text{res}}\phi_{\text{res}} = \Omega - \phi_m^T\bar{K}\phi_m\\ &= \Omega - \phi_m^T\left[\phi_m\Omega^{-1}\phi_m^T\right]^{-1}\phi_m\end{aligned} \tag{A10}$$

Note that $\Delta\Omega$ is a function solely of ϕ_m and Ω.

To determine $\hat{K}$ and $\hat{M}$ from Eq. (A9), we must augment the measured mode shapes by a vector basis for the unknown mode shape partition ϕ_{res}. The required minimal rank augmentation of ϕ_m is determined through the dynamic residual matrix $\Delta\Omega$. To find the rank of Ω_{res} and a vector basis for ϕ_{res}, we utilize a singular value decomposition (SVD) of $\Delta\Omega$, viz.,

$$PSP^T = \text{SVD}(\Delta\Omega) \tag{A11}$$

Examination of the singular values indicates the required dimension of the augmented coordinates ξ. For example, with l spatial measurements, $\phi_m^T\bar{K}\phi_m$ will typically be of rank l, whereas Ω is rank n, and $\Delta\Omega$ is rank $n-l$. Therefore, the SVD should determine $n-l$ nonzero singular values for $\Delta\Omega$. It is possible, however, for the reduced matrix to exhibit rank deficiency (for example, if flexibility mode contributions to $\bar{K}$ are updated to account for rigid-body modes), and so a rigorous approach examines the singular values of $\Delta\Omega$ to determine the correct rank p,

$$\Delta\Omega = PSP^T = P_pS_pP_p^T \tag{A12}$$

Having determined a basis P_p for the augmented coordinates, we now augment ϕ_m by the rows of P_p^T which span the singular values and solve the inverse problem

$$\begin{aligned}\begin{bmatrix}\bar{K} & 0\\ 0 & K_{\text{res}}\end{bmatrix} &= \begin{bmatrix}\phi_m\\ P_p^T\end{bmatrix}^{-T}\Omega\begin{bmatrix}\phi_m\\ P_p^T\end{bmatrix}^{-1}\\ \begin{bmatrix}\bar{M} & \bar{M}_c\\ \bar{M}_c^T & M_{\text{res}}\end{bmatrix} &= \begin{bmatrix}\phi_m\\ P_p^T\end{bmatrix}^{-T}\Omega\begin{bmatrix}\phi_m\\ P_p^T\end{bmatrix}^{-1}\end{aligned} \tag{A13}$$

Finally, the augmented DOF are orthonormalized by solving the generalized eigenproblem

$$\begin{aligned}K_{\text{res}}U &= M_{\text{res}}U\Omega_\xi\\ U^TK_{\text{res}}U &= \Omega_\xi\\ U^TM_{\text{res}}U &= I\end{aligned} \tag{A14}$$

and performing a final transformation on the mass and stiffness matrices

$$\begin{aligned}\hat{K} &= \begin{bmatrix}\bar{K} & 0\\ 0 & U^TK_{\text{res}}U\end{bmatrix} = \begin{bmatrix}\bar{K} & 0\\ 0 & \Omega_\xi\end{bmatrix}\\ \hat{M} &= \begin{bmatrix}\bar{M} & \bar{M}_cU\\ U^T\bar{M}_c^T & U^TM_{\text{res}}U\end{bmatrix} = \begin{bmatrix}\bar{M} & M_c\\ M_c^T & I\end{bmatrix}\end{aligned} \tag{A15}$$

Thus, in a mathematical sense, $[\hat{K}, \hat{M}]$ is an equivalent measure of the normal mode parameters as observed from physical DOF $\boldsymbol{q}_m$. Furthermore, this realization is unique from its definition in terms of the modal parameters of the system. Note also that the definitions of $\hat{K}$ and $\hat{M}$ include as special cases both the modal model $[\Omega, I]$ and the physical model $[K, M]$ in the limits as the number of measured DOF varies from 0 to n.

Appendix B: Assembly of the Global Structure from Identified Substructures

As already stated, we utilize the minimal-order mass and stiffness representation of the identified substructures to synthesize the global structural model. To this end, we begin with N_{sub} substructure identifications from which the normal modal parameters are extracted. To enhance the substructure identification, we utilize a particularly efficient implementation of the ERA algorithm,[15] which allows for extremely large data sets and thus enhances the ability to accurately obtain higher order observable modes. Then, utilizing the procedure in the preceding section, we can construct the minimal-order stiffness and mass matrices for each substructure. Therefore, the identified second-order equations of motion for each uncoupled substructure j is given by

$$\begin{aligned}&\begin{bmatrix}\bar{M}_{bb} & \bar{M}_{bi} & M_{bc}\\ \bar{M}_{bi}^T & \bar{M}_{ii} & M_{ic}\\ M_{bc}^T & M_{ic}^T & I\end{bmatrix}_{(j)}\begin{bmatrix}\ddot{\boldsymbol{q}}_m\\ \ddot{\boldsymbol{q}}_i\\ \ddot{\xi}\end{bmatrix}_{(j)} + \begin{bmatrix}\bar{D}_{bb} & \bar{D}_{bi} & D_{bc}\\ \bar{D}_{bi}^T & \bar{D}_{ii} & D_{ic}\\ D_{bc}^T & D_{ic}^T & \Xi_\xi\end{bmatrix}_{(j)}\\ &\times\begin{bmatrix}\dot{\boldsymbol{q}}_m\\ \dot{\boldsymbol{q}}_i\\ \dot{\xi}\end{bmatrix}_{(j)} + \begin{bmatrix}\bar{K}_{bb} & \bar{K}_{bi} & 0\\ \bar{K}_{bi}^T & \bar{K}_{ii} & 0\\ 0 & 0 & \Omega_\xi\end{bmatrix}_{(j)}\begin{bmatrix}\boldsymbol{q}_m\\ \boldsymbol{q}_i\\ \xi\end{bmatrix}_{(j)} = \begin{bmatrix}f_b\\ f_i\\ 0\end{bmatrix}_{(j)}\end{aligned} \tag{B1}$$

where $\boldsymbol{q}_{b(j)}$ are the physical boundary DOF which are measured for each substructure, $\boldsymbol{q}_{i(j)}$ are additional physical DOF for the minimal-order matrices that are not at the substructure boundary, and $\xi_{(j)}$ are the generalized augmented DOF of the minimal-order substructure representation which preserve the equivalence of Eq. (B1) to the given system realization.

To synthesize the global equations of motion, displacement compatibility and equilibrium at the boundary are imposed, viz.,

$$\boldsymbol{q}_{b(j)} = \boldsymbol{q}_b, \quad j = 1, \ldots, N_{\text{sub}} \quad \text{and} \quad \sum_{j=1}^{N_{\text{sub}}} f_{b(j)} = f_b \tag{B2}$$

which leads to the assembled equations of motion

$$\begin{aligned}&\begin{bmatrix}\bar{M}_{bb} & \bar{M}_{bi} & M_{bc}\\ \bar{M}_{bi}^T & \bar{M}_{ii} & M_{ic}\\ M_{bc}^T & M_{ic}^T & I\end{bmatrix}\begin{bmatrix}\ddot{\boldsymbol{q}}_b\\ \ddot{\boldsymbol{q}}_i\\ \ddot{\xi}\end{bmatrix} + \begin{bmatrix}\bar{D}_{bb} & \bar{D}_{bi} & D_{bc}\\ \bar{D}_{bi}^T & \bar{D}_{ii} & D_{ic}\\ D_{bc}^T & D_{ic}^T & \Xi_\xi\end{bmatrix}\begin{bmatrix}\dot{\boldsymbol{q}}_b\\ \dot{\boldsymbol{q}}_i\\ \dot{\xi}\end{bmatrix}\\ &+ \begin{bmatrix}\bar{K}_{bb} & \bar{K}_{bi} & 0\\ \bar{K}_{bi}^T & \bar{K}_{ii} & 0\\ 0 & 0 & \Omega_\xi\end{bmatrix}\begin{bmatrix}\boldsymbol{q}_b\\ \boldsymbol{q}_i\\ \xi\end{bmatrix} = \begin{bmatrix}f_b\\ f_i\\ 0\end{bmatrix}\end{aligned} \tag{B3}$$

where the matrix partitions are given by

$$\bar{M}_{bb} = \sum_{j=I}^{N_{\text{sub}}} \bar{M}_{bb(j)} \qquad \bar{D}_{bb} = \sum_{j=I}^{N_{\text{sub}}} \bar{D}_{bb(j)}$$

$$\bar{K}_{bb} = \sum_{j=I}^{N_{\text{sub}}} \bar{K}_{bb(j)}$$

$$\bar{M}_{bi} = [\bar{M}_{bi(I)} \quad \bar{M}_{bi(II)} \quad \cdots \quad \bar{M}_{bi(N)}]$$

$$M_{bc} = [M_{bc(I)} \quad M_{bc(II)} \quad \cdots \quad M_{bc(N)}]$$

$$\bar{M}_{ii} = \begin{bmatrix} \bar{M}_{ii(I)} & 0 & \cdots & 0 \\ 0 & \bar{M}_{ii(II)} & \cdots & 0 \\ \vdots & \vdots & \vdots & \vdots \\ 0 & 0 & \cdots & \bar{M}_{ii(N)} \end{bmatrix}$$

$$M_{ic} = \begin{bmatrix} M_{ic(I)} & 0 & \cdots & 0 \\ 0 & \bar{M}_{ic(II)} & \cdots & 0 \\ \vdots & \vdots & \vdots & \vdots \\ 0 & 0 & \cdots & \bar{M}_{ic(N)} \end{bmatrix}$$

$$\bar{D}_{bi} = \begin{bmatrix} \bar{D}_{bi(I)} & \bar{D}_{bi(II)} & \cdots & \bar{D}_{bi(N)} \end{bmatrix}$$

$$D_{bc} = \begin{bmatrix} D_{bc(I)} & D_{bc(II)} & \cdots & D_{bc(N)} \end{bmatrix} \tag{B4}$$

$$\bar{D}_{ii} = \begin{bmatrix} \bar{D}_{ii(I)} & 0 & \cdots & 0 \\ 0 & \bar{D}_{ii(II)} & \cdots & 0 \\ \vdots & \vdots & \vdots & \vdots \\ 0 & 0 & \cdots & \bar{D}_{ii(N)} \end{bmatrix}$$

$$D_{ic} = \begin{bmatrix} D_{ic(I)} & 0 & \cdots & 0 \\ 0 & \bar{D}_{ic(II)} & \cdots & 0 \\ \vdots & \vdots & \vdots & \vdots \\ 0 & 0 & \cdots & \bar{D}_{ic(N)} \end{bmatrix}$$

$$\Xi_{\xi} = \begin{bmatrix} \Xi_{\xi(I)} & 0 & \cdots & 0 \\ 0 & \bar{\Xi}_{\xi(II)} & \cdots & 0 \\ \vdots & \vdots & \vdots & \vdots \\ 0 & 0 & \cdots & \bar{\Xi}_{\xi(N)} \end{bmatrix}$$

$$\Omega_{\xi} = \begin{bmatrix} \Omega_{\xi(I)} & 0 & \cdots & 0 \\ 0 & \bar{\Omega}_{\xi(II)} & \cdots & 0 \\ \vdots & \vdots & \vdots & \vdots \\ 0 & 0 & \cdots & \bar{\Omega}_{\xi(N)} \end{bmatrix}$$

and the internal displacement and force vectors are defined as

$$q_i = \begin{bmatrix} q_{i(I)} \\ q_{i(II)} \\ \vdots \\ q_{i(N_{\text{sub}})} \end{bmatrix} \qquad \xi_i = \begin{bmatrix} \xi_{(I)} \\ \xi_{(II)} \\ \vdots \\ \xi_{(N_{\text{sub}})} \end{bmatrix} \qquad f_i = \begin{bmatrix} f_{i(I)} \\ f_{i(II)} \\ \vdots \\ f_{i(N_{\text{sub}})} \end{bmatrix} \tag{B5}$$

by solving the generalized undamped eigenvalue problem.

The present procedure is straightforward once the minimal-order mass and stiffness representations of the individual substructures have been obtained. The assembly procedure is, in fact, identical to the displacement-method-based construction of global matrices in the finite element method, and thus many existing finite element packages could be extended to allow assembly of test-measured substructure models, including integration into analytical finite element models.

Acknowledgments

This research was sponsored in part by NASA Grant NAG-1-1200 and gifts from Shimizu Corporation and the McDonnell Douglas Foundation. The authors would like to thank our undergraduate assistants at the McDonnell Douglas Structural Dynamics and Controls Laboratory at the University of Colorado, Boulder, for their testing support, in particular, Nikki Robinson and Stephanie Gow.

References

[1]Coppolino, R. N., "Employment of Hybrid Experimental/ Analytical Modeling in Component Mode Synthesis of Aerospace Structures," Colloquium on Combined Experimental/Analytical Modeling of Dynamic Structural Systems using Substructure Synthesis, Joint ASME/ASCE Applied Mechanics Conf., Albuquerque, NM, June 1985.

[2]Craig, R. R., and Bampton, M. C., "Coupling of Substructures for Dynamic Analyses," *AIAA Journal*, Vol. 6, No. 7, 1968, pp. 1313–1319.

[3]Yang, C.-D., and Yeh, F.-B., "Identification, Reduction, and Refinement of Model Parameters by the Eigensystem Realization Algorithm," *Journal of Guidance, Control, and Dynamics*, Vol. 13, No. 6, 1990, pp. 1051–1059.

[4]Su, T.-J., and Juang, J.-N., "Substructure System Identification and Synthesis," *Proceedings of the 34th Structures, Structural Dynamics, and Materials Conference* (La Jolla, CA), AIAA, Washington, DC, 1993 (AIAA Paper 93-1649).

[5]Martinez, D. R., Miller, A. K., and Carne, T. G., "Combined Experimental/Analytical Modeling of Shell/Payload Structures," Sandia National Lab., Rept. SAND84-2598, Dec. 1985.

[6]Alvin, K. F., Peterson, L. D., and Park, K. C., "Method for Determining Minimum-Order Mass and Stiffness Matrices from Modal Test Data," *AIAA Journal*, Vol. 33, No. 1, 1995, pp. 128–135.

[7]Ewins, D. J., *Modal Testing: Theory and Practice*, Research Studies Press Ltd., 1984.

[8]Bendat, J. S., and Piersol, A. G., *Engineering Applications of Correlation and Spectral Analysis*, 2nd ed., Wiley-Interscience, New York, 1993.

[9]Juang, J. N., and Pappa, R. S., "An Eigensystem Realization Algorithm for Modal Parameter Identification and Model Reduction," *Journal of Guidance, Control, and Dynamics*, Vol. 8, No. 5, 1985, pp. 620–627.

[10]Peterson, L. D., and Alvin, K. F., "A Time and Frequency Domain Procedure for Identification of Structural Dynamic Models," *Proceedings of the 36th Structures, Structural Dynamics, and Materials Conference* (Hilton Head, SC), AIAA, Washington, DC, 1994 (AIAA Paper 94-1731).

[11]Alvin, K. F., and Park, K. C., "Second-Order Structural Identification Procedure via State Space-Based System Identification," *AIAA Journal*, Vol. 32, No. 2, 1994, pp. 397–406.

[12]Alvin, K. F., "Second-Order Structural Identification via State Space-Based System Realizations," Ph.D. Thesis, Univ. of Colorado, CU-CSSC-93-09, Center for Aerospace Structures, Boulder, CO, 1993.

[13]Hurty, W. C., "Dynamic Analysis of Structural Systems Using Component Modes," *AIAA Journal*, Vol. 3, 1965, pp. 678–685.

[14]Guyan, R. J., "Reduction of Stiffness and Mass Matrices," *AIAA Journal*, Vol. 3, No. 2, 1965, p. 380.

[15]Peterson, L. D., "Efficient Computation of the Eigensystem Realization Algorithm," *Journal of Guidance, Control, and Dynamics*, Vol. 18, No. 3, 1995, pp. 395–403.